Molecular clouds at the edge of the Galaxy: Clouds of FOG

J.G.A. Wouterloot[1], J. Brand[2]
[1]I. Physikalisches Institut, Universität zu Köln, 50937 Köln, Germany
[2]Istituto di Radioastronomia CNR, 40129 Bologna, Italy

I. Introduction

The outer Galaxy (defined as those parts of the Galaxy with $R>R_0=8.5$ kpc) in general and particularly the outermost regions ($R \gtrsim 16$ kpc; which we shall refer to as the far-outer Galaxy [FOG]) has not received the observational attention that has been dedicated to the inner Galaxy and the solar neighbourhood. Notable exceptions to this are a.o. studies of HI (e.g. Kulkarni et al. 1982, Henderson et al. 1982), in which its distribution and kinematic properties have been analyzed out to R=20-30 kpc (kinematic distance). The reason for this lack of attention is quite obvious: most of the molecular clouds and stars are inside $R \approx 12$ kpc. Kutner & Mead (1981) were the first to specifically make a molecular survey of (a section of) the outer Galaxy, and they found relatively widespread CO emission with kinematic distances corresponding to R up to about 23 kpc. They subsequently mapped some of the clouds with $R<13$ kpc in CO (Mead & Kutner 1988, hereafter MK88) and derived their masses, luminosities, and temperatures. Several other studies of individual outer Galaxy molecular clouds were carried out as well [Carpenter et al. 1990 (CSS90); Digel 1991 (Dig91); Sodroski 1991 (Sodr91)], but all of these are at $R \lesssim 14$ kpc. The objects mapped by Dig91 and MK88 are located in a region called the Outer Arm, which might either be a separate spiral arm or be connected to the Perseus Arm in the second quadrant (see figure 1 of Henderson et al. 1982). Apart from the Perseus Arm there are no known optical spiral arms in the outer Galaxy with the possible exception of a collection of optical tracers 1 or 2 kpc beyond the Perseus Arm, which may define a spiral arm segment (Kimeswenger & Weinberger 1989). Henderson et al. (1982) connect the Perseus Arm to emission in the third quadrant, but the justification for this is weak.

In order to extend our understanding of the processes that lead to the formation of clouds and stars under physical conditions that are quite different from those found in the solar neighbourhood and in the inner Galaxy, it is however important to identify and study molecular clouds and embedded star forming regions at still larger R. In very general terms one could say that most things one finds in the inner Galaxy are also present in the far-outer Galaxy, but there is much less of it. To give some specific examples: The HI and H_2 gas surface and volume densities are much smaller, and their scale-heights are larger (Wouterloot et al. 1990); the star density is much smaller, there is less star formation; the interstellar radiation field (ISRF) is much weaker (Mathis et al. 1983; Bloemen 1985); there are no (known) spiral arms and fewer SNR's, so there are fewer and/or weaker external triggers for cloud- and star formation; He and metal abundances are lower (Shaver et al. 1983; Wilson & Matteucci 1992, hereafter WM92);

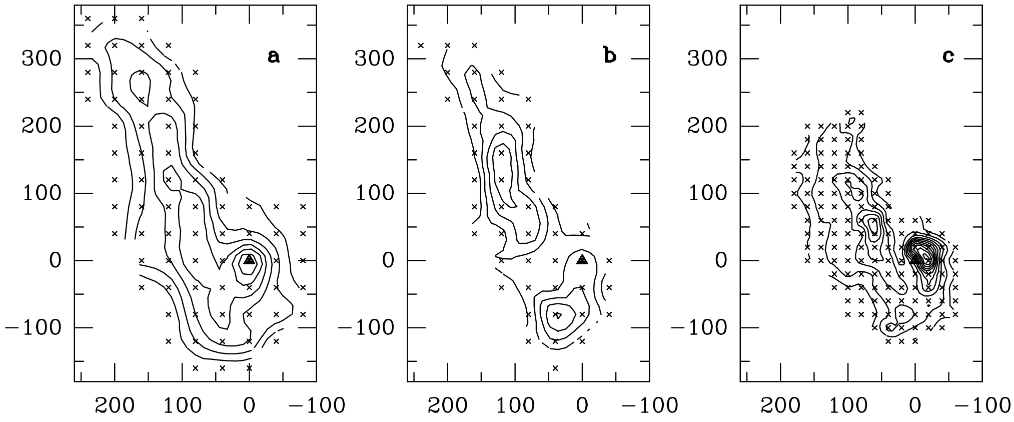

Figure 1: *Distribution of peak T_{mb} of WB1152 obtained with the SEST. a) $^{12}CO(1\text{–}0)$; contour levels are 1(1)K. b) $^{13}CO(1\text{–}0)$; 0.2(0.2)K. c) $^{12}CO(2\text{–}1)$; 1(1)K. The triangle indicates the position of IRAS08282−4545. Offset in arcsec in RA, Dec.*

the FIR emissivity is smaller (Deul 1988), and the pressure of the intercloud medium is much smaller (Elmegreen 1989). This changing environment is expected to have its influence on cloud- and star formation.

This paper therefore deals with star-forming molecular clouds at the edge of the galactic - or more specifically the molecular - disk: where the edge is located depends on the tracer one uses. Atomic hydrogen has been found out to kinematic distances of 25 to 30 kpc from the center (e.g. Kulkarni et al. 1982). From CCD photometry towards l=180°, b=2.8°, Robin et al. (1992a,b) conclude that the edge of the stellar disk is between 5.5 and 6 kpc from the Sun at about 14-15 kpc from the galactic center. Carney & Seitzer (1993) found indications for stars in one out of four fields located in the galactic warp at l=277°, b=−4.2° at R=16-17 kpc. Theoretical estimates of the location of the edge of the Galaxy depend on the value for the disk scale-length and thickness at R=8.5 kpc (van der Kruit 1986). This scale-length is 2.2-5.5 kpc (Robin et al. 1992b) which suggests a location of the optical edge of the Galaxy at R<21 kpc (Carney & Seitzer 1993). The scale-lengths found at R>13 kpc by Wouterloot et al. (1990) are somewhat smaller: 1.5 kpc for molecular clouds and 1.9 kpc for HII regions. They found the value for the HI gas to be 4.0 kpc.
Optically visible HII regions with (spectro-) photometrically determined distances have been found out to R≈16-17 kpc (Moffat et al. 1979; Fich et al. 1989; Turbide & Moffat 1993; Brand & Blitz 1993). Wouterloot & Brand (1989; hereafter WB89) find star-forming molecular clouds out to R_{kin} ≈20 kpc (the HII region S266 has R_{kin} ≈19 kpc). The optical edge of the galactic disk is therefore located somewhere between 16 and 20 kpc from the galactic center, and this range also defines the edge of the molecular disk. Very recently an optical HII region was found, associated with a molecular cloud at R≈28 kpc (de Geus et al. 1993; Digel et al. 1994). The ionizing star has presumably been identified and its spectrophotometric distance, although uncertain, puts it

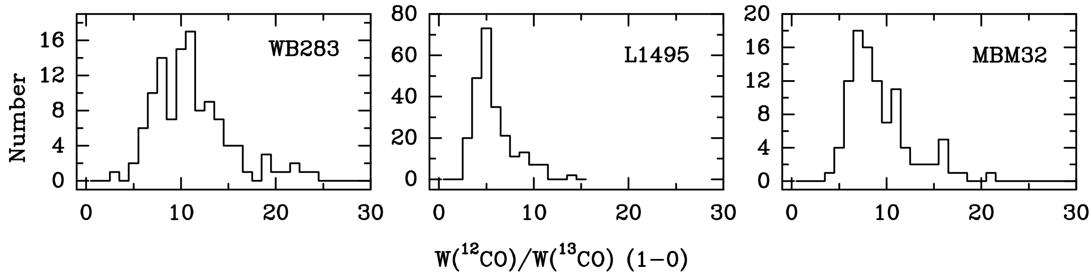

Figure 2: *Histogram of the ratio W[^{12}CO(1-0)]/W[^{13}CO(1-0)] for the FOG cloud WB283, for a dark cloud in the solar neighbourhood (L1495), and for a high latitude cloud (MBM32).*

at $24.5 \lesssim R \lesssim 39$ kpc.

WB89 colour-selected IRAS sources with a FIR spectral distribution typical of star-forming regions from the Point Source Catalogue, and used them as tracers for the molecular gas. More than 1000 molecular clouds with embedded heating sources, and with R>8.5 kpc were found, of which almost 200 are at R>14 kpc. Brand & Wouterloot (1994a; hereafter BW94) mapped 27 clouds from the WB89 sample in ^{12}CO (1–0), and observed several other CO isotopes and -transitions at selected positions. The clouds in this sample have galactocentric distances $15.7<R_{kin}<20.2$ kpc (see Table 8 in BW94), with an average R of 17.3±1.2 kpc (1 σ); the median R is 16.8 kpc. We adopt 17 kpc as a representative value. An example of the results of the observations of one of the clouds is shown in Fig. 1.

In the present paper we analyze these data, comparing the results with those derived from similar observations of inner Galaxy clouds taken from the literature, and we try to use this to quantify differences in the various physical parameters (e.g. masses, kinetic temperature, and molecular abundances) between the inner- and far-outer Galaxy that are a result of the changing environment (see Brand & Wouterloot 1994b for an extensive analysis).

II. Cloud Temperatures

A simple molecular cloud consists of a (dense) core, which has an approximately constant temperature, and an envelope, where the temperature increases outwards. Giant molecular clouds or -complexes (GMCs) can be thought of as a collection of cores with their envelopes, embedded in a layer of warm lower-density gas, which is part atomic, part molecular. The heating of the envelope and the inter-clump gas is dominated by the interstellar radiation field, which however in the far-outer Galaxy is probably negligible, although with the present knowledge it is not possible to make a quantitative statement. The cores are heated mostly by cosmic rays; cooling takes places through molecular line emission. For two clouds for which we have observations in up to five ^{12}CO and ^{13}CO transitions we have used escape probability models to derive a T_{kin} in the range 10 to 18 K, consistent with observations of inner Galaxy clouds, which show

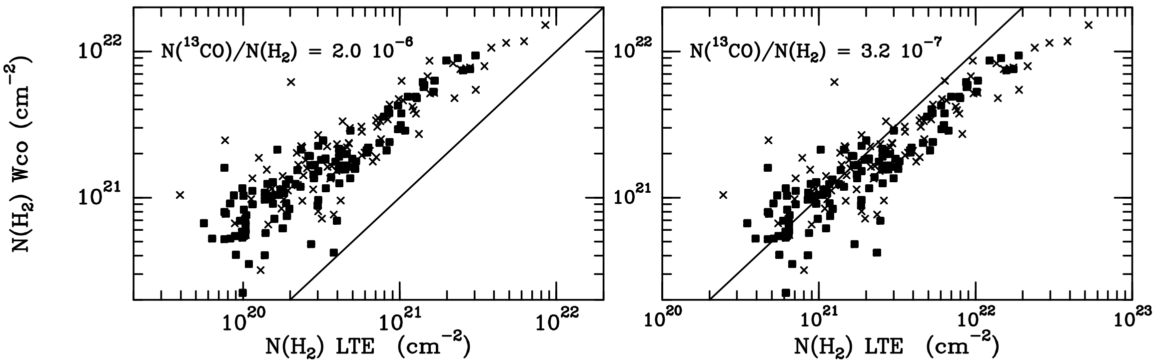

Figure 3: *Comparison of column densities of H_2 calculated via $N_{W_{CO}} = X\, W_{CO}$, with N_{lte}. The filled squares are IRAM 30-m data of the WB283 cloud and the crosses SEST data of several other FOG clouds. Left-hand panel: used local abundance ratio N(^{13}CO)/N(H_2); right-hand panel: used abundance ratio at R=17 kpc, extrapolated from the gradients given by WM92. In both panels X=2.3 10^{20} $cm^{-2}(Kkms^{-1})^{-1}$, i.e. the value appropriate for local GMCs, and the drawn line is for equal column densities. When taking the abundance gradients into account $N_{W_{CO}} \approx N_{lte}$ for X in the far-outer Galaxy equal to the local value.*

similar line ratios and from which a T_{kin} of 10 to 15 K was derived (Sanders et al. 1993). In addition we find, from a statistical analysis of measured antenna temperatures of fore- and background clouds in WB89, that the average T_A^* of ^{12}CO(1-0) does not depend on R in the range 9-16 kpc. Although the sources of cosmic rays (supernovae, pulsars) are strongly concentrated towards the central region of the disk, gamma ray observations are consistent with the existence of a cosmic ray halo (Bloemen 1989; Dogiel 1991). This might well explain the observed lack of temperature difference between inner- and outer Galaxy clouds.

III. Cloud masses

One way to determine masses from ^{12}CO(1-0) data alone is to make use of the empirical fact that, at least for local GMCs, there is a constant ratio X = $[N(H_2)/\int T dv] \approx (2.3 \pm 0.3)10^{20}$ $cm^{-2}(Kkms^{-1})^{-1}$ (Strong et al. 1988). The resulting column density we shall call $N_{W_{CO}}$ ($W_{CO} \equiv \int T dv$) and the mass derived from this $M_{W_{CO}}$. For about 200 lines-of-sight towards our far-outer Galaxy clouds we have both ^{12}CO and ^{13}CO data. For one of the FOG clouds mapped with the 30-m IRAM telescope, we show a comparison of the observed ratios of $\int T dv$ of both isotopes with that in local clouds in Fig. 2. The median values are about 10 (WB283), 5 (L1495), and 9 (MBM32). We think that the high value for the FOG is caused by the lower ^{13}CO abundance rather than a low ^{12}CO optical depth as is the case in the high latitude cloud MBM32. From these data we derive LTE-column densities (N_{lte}; mass M_{lte}) and compare these to $N_{W_{CO}}$ in Fig. 3. In the left-hand panel we used the local abundance ratio for N(^{13}CO)/N(H_2)=2.0 10^{-6} (Dickman 1978) when calculating N_{lte}, while in the right-hand panel we used the abundance ratio extrapolated to R=17 kpc (the average R

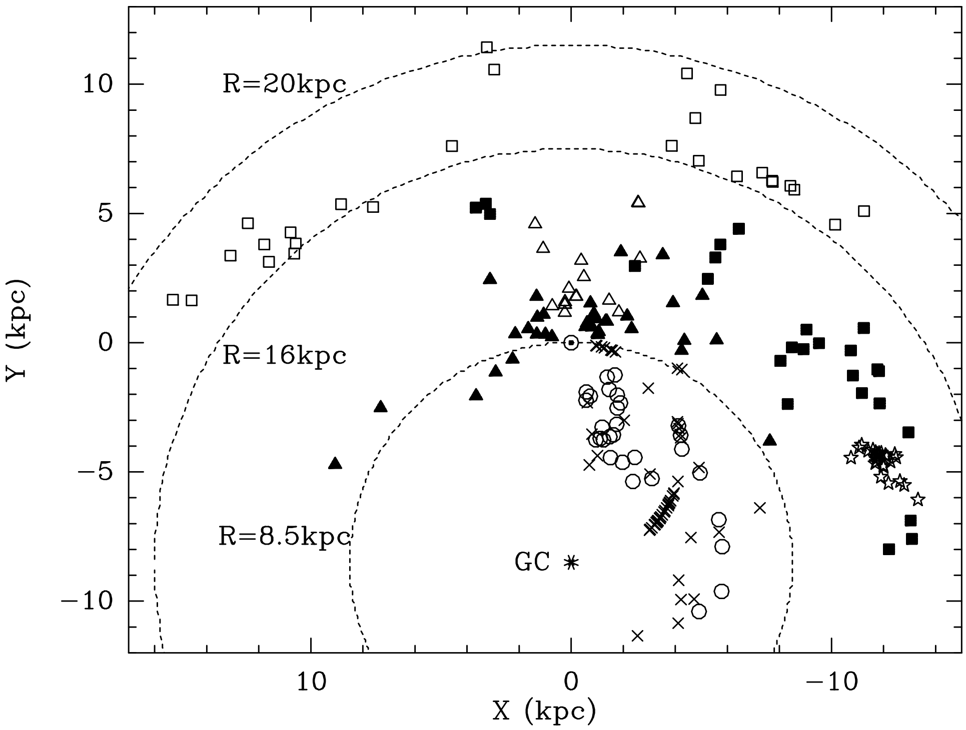

Figure 4: *Distribution of the molecular clouds in the extended data set, projected onto the galactic plane. The Sun is at (X,Y)=(0,0), and indicated by ⊙; the galactic center is at (X,Y)=(0,−8.5). Dashed circle segments indicate R=8.5, 16, and 20 kpc respectively. The individual data sets are distinguished by different symbols: BW94 (open squares), MK88 (filled squares), CSS90 (open triangles), Sodr91 (filled triangles), Dig91 (asterisks), Dame et al. 1986 (Dame86, circles), Solomon et al. 1987 (crosses).*

of our sample), 3.2 10^{-7}, using the gradients given in WM92 for [^{12}C]/[H] and [^{12}C]/[^{13}C]. It is clear that when taking into account the galactic abundance gradient, both column densities are approximately equal, and the median value of X which one would derive from N_{lte}/W_{CO} is 2.9 10^{20} cm^{-2}(Kkms^{-1})$^{-1}$ [with an rms deviation for individual *positions* of about 1.5 10^{20} cm^{-2}(Kkms^{-1})$^{-1}$], which is close to the assumed value of 2.3 10^{20} cm^{-2}(Kkms^{-1})$^{-1}$. This finding is in contrast to that of previous studies (e.g. MK88, Dig91, Sodr91) who all argue for a value of X in the outer Galaxy which is 2.5 – 4 times larger than the local value, based on a comparison of inner- and outer Galaxy cloud luminosities and virial masses.

To investigate this in more detail we have combined our data set with data on outer Galaxy clouds taken from the literature (see caption of Fig. 4), making sure to scale all distances and masses to the same system, which resulted in a collection of 130 clouds with 8.5 $\lesssim$ R $\lesssim$ 20 kpc. In addition we collected data on 92 inner Galaxy clouds from the literature for which the derived parameters were also scaled with the same assumptions. The distribution projected onto the galactic plane of these clouds is shown in Fig. 4. Distinguishing between clouds at R smaller or larger than 8.5 kpc,

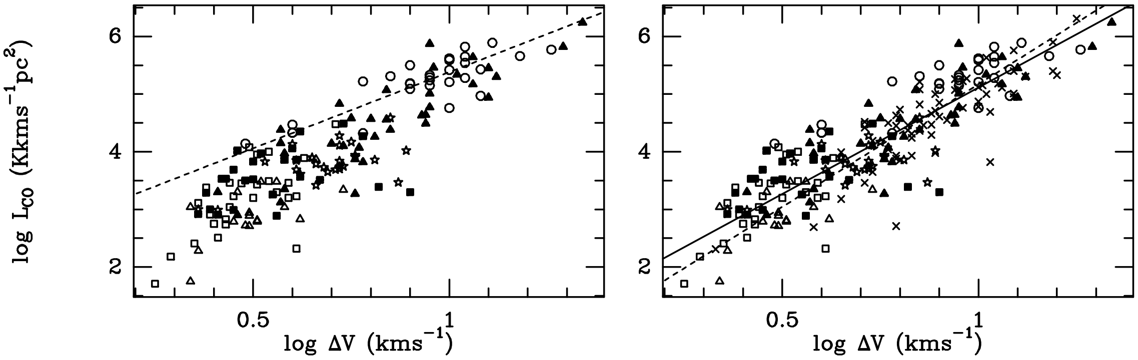

Figure 5: **a.** *Log L_{CO} versus log Δv for all outer Galaxy clouds from the combined sample and the Dame86 inner Galaxy clouds. The dashed line is a least squares fit through the latter points. Symbols are as in Fig. 4.* **b.** *The same as a., but showing all inner Galaxy clouds. The drawn line is a least-squares fit through the outer Galaxy data only; the dashed line fits the inner Galaxy data.*

we show in Fig. 5 a plot of cloud luminosity L_{CO} versus linewidth. Since both quantities are independent of the beamsize, one does not expect any systematic differences between the various surveys. Taking only the Dame86 data for the inner Galaxy there seems to be a considerable difference compared to the outer Galaxy (Fig. 5a). Dig91 concluded from similar data that the ratio X is a factor of 4 larger in the outer Galaxy, because $L_{CO} \propto M_{Wco}/X$, and assuming $M_{Wco}=M_{vir}$ ($\Delta v \propto \sqrt{M_{vir}}$). However least-squares fits through all inner Galaxy or all outer Galaxy data (see Fig. 5b) are essentially identical.

A comparison of Fig. 5a and 5b suggests that the conclusion of Dig91 was caused by the small number of small (i.e. low mass and low luminosity) clouds included in the inner Galaxy sample (which biases the inner Galaxy fit) and that there is no need for a sudden change of X at R_0, which confirms our conclusion based on the analysis of LTE column densities.

The distribution of cloud mass with R is shown in Fig. 6a. It is seen that in surveys of the inner Galaxy clouds of mass less than about 3 10^4 $M_\odot$ are missing, probably because of confusion. In the far-outer Galaxy there are no very massive clouds. We think that this is due to the small number of clouds in the sample. Assuming that the distribution over mass is the same for both samples and combining the data at some intermediate mass, we have binned the clouds in mass, fitted a power law to the resulting mass spectrum, and obtained $dN/dM_{Wco} \propto M_{Wco}{}^{-1.90\pm0.11}$. A similar exercise applied only to the outer Galaxy clouds gives a slope of -1.48 ± 0.12. These mass spectra are consistent with those found for other samples of local and inner Galaxy clouds as well as with those found for clumps within molecular clouds, and this gives important information on cloud- and clump formation scenarios. These spectra are in fact what one expects when GMCs grow via accretion and coalescence of smaller

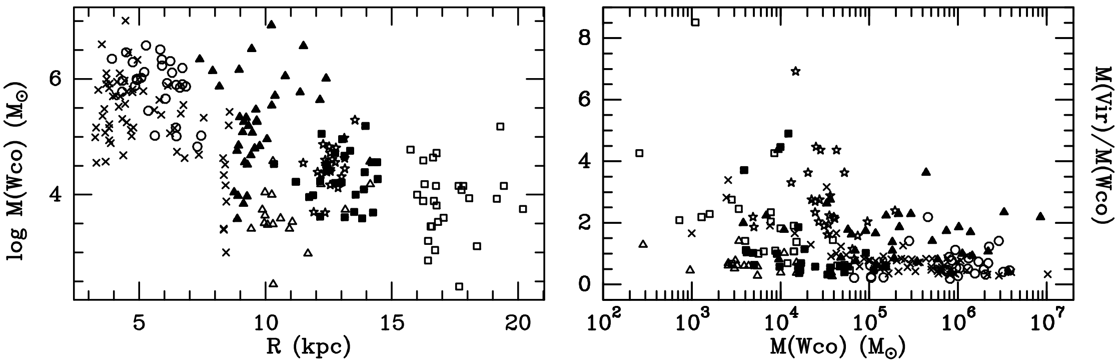

Figure 6: **a.** *Plot of M_{Wco} versus R for clouds in the combined data set.* **b.** *The ratio of virial mass and M_{Wco} as a function of the latter. Symbols are as in Fig. 4.*

clouds (Combes 1991). If one integrates the mass function up to 10^7 $M_\odot$, the total mass of molecular clouds in the outer Galaxy is 9.6 10^6 $M_\odot$.

The ratio of virial mass ($=126$ r Δv^2) and M_{Wco} as a function of M_{Wco} for the combined sample is shown in Fig. 6b. This ratio ranges between 0.28 and 8.5, and the median value decreases from 1.69 for 10^2 -10^3 $M_\odot$ to 0.61 for 10^6 -10^7 $M_\odot$. Note that because of the assumption $\rho \propto r^{-2}$, the virial mass is a lower limit. The more massive clouds are situated in the inner Galaxy (see Fig. 6a); however the work of Adler & Roberts (1992) shows that clouds which seemingly are real entities, in reality may consist of clouds located along the line of sight over several kpc, and are therefore not always gravitationally bound objects.

IV. Systematic motions

The line width $\Delta v_{\rm comp}$ of the composite spectrum (the sum of all spectra) of a molecular cloud is the result of random and systematic motions. The amount of small-scale random motion is represented by the average linewidth $<\Delta v>$ of all individual spectra, while the systematic component is characterized by the dispersion $\sigma_{\rm sys}$ around the average $V_{\rm lsr}$ of all detections: $\Delta v_{\rm comp} = \sqrt{(<\Delta v>^2 + [2.35\sigma_{\rm sys}]^2)}$.

We have compared the random- and systematic components in the 27 clouds observed by us (BW94; see Fig. 7). Most clouds have a random component which is larger than the systematic one, but four clouds have $\Delta v_{\rm sys} > \Delta v_{\rm rand}$. For a number of clouds we have determined the direction along which the gradient is largest in one coordinate, while being smallest in the other. Spectra were then summed in strips perpendicular to the direction of the gradient, and gauss fits were made to the sum spectra to get the velocity of the peak of the emission at each position along its direction. Interpreting this as being due to (solid body) rotation we have thus derived a.o. the angle of the rotation axis with respect to the (equatorial) coordinate system in which the observations were made, and the magnitude of the gradient, which has values between 0.018 and 0.266 $\rm kms^{-1}pc^{-1}$. A typical value for local GMCs is $\lesssim$ 0.05 $\rm kms^{-1}pc^{-1}$ (Blitz 1991).

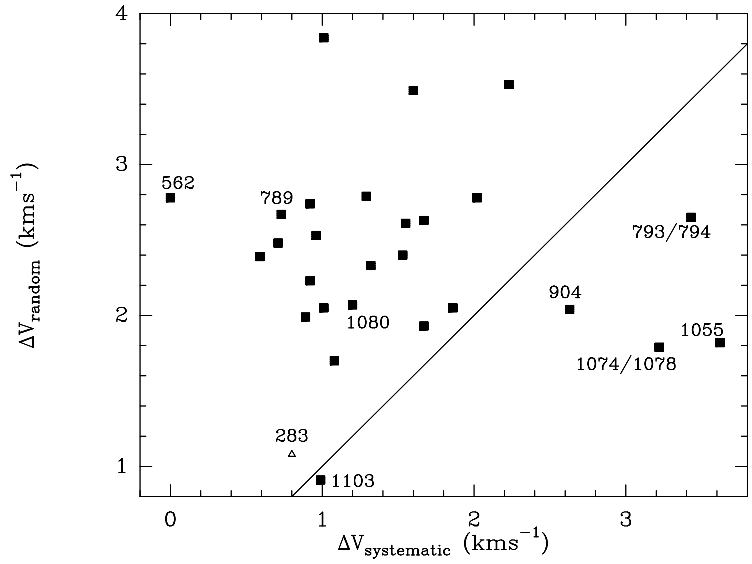

Figure 7: *Comparison of random and systematic velocity components in FOG clouds. The random component of a cloud is derived from the average of all line widths, while the systematic component is characterized by the dispersion around the average V_{lsr} of the peak of the emission. The drawn line indicates equal contributions. Some clouds are identified by their number from WB89.*

V. Conclusions

• The line ratios of different CO transitions (except $^{12}CO/^{13}CO$) in the FOG are similar to those in the inner Galaxy. Using escape probability models we derive kinetic temperatures of the clouds which are in the same range for both parts of the Galaxy.
• Between R=9-16 kpc there is no change in the mean observed T_A^* of mapped clouds and of clouds happening to be along the line of sight towards IRAS point sources. If this T_A^* is related to the kinetic temperatures of these clouds, this would suggest that if there is a population of very cold clouds in the FOG as recently proposed by Lequeux et al. (1993), it is not detected in normal surveys or the relative number of such clouds is not depending on R.
• Assuming that the average galactic abundance gradients can be extrapolated to R=17 kpc, we derive from LTE calculations a median value of X=2.9 10^{20} cm^{-2} (Kkms^{-1})$^{-1}$, close to the value derived by Strong et al. (1988) for the inner Galaxy. Previous suggestions that X is larger in the outer Galaxy by a factor of 2.5-4 are wrong due to small number statistics.
• The mass spectrum of outer Galaxy clouds (slope ≈ -1.48) is approximately the same as that of inner Galaxy clouds. Combining both samples gives a slope of -1.90.
• At least 20% of the FOG clouds show significant velocity gradients, comparable to those found in local clouds.

References:

Adler D.S., Roberts W.W.: 1992 ApJ 384, 95

Blitz L.: 1991, in: Lada C.J. & Kylafis N.D. (eds), The Physics of Star Formation and Early Stellar Evolution, p. 3

Bloemen J.B.G.M.: 1985 A&A 145, 391

Bloemen J.B.G.M.: 1989 ARA&A 27, 469

Brand J., Blitz L.: 1993 A&A 275, 67

Brand J., Wouterloot J.G.A.: 1994a A&AS *in press*

Brand J., Wouterloot J.G.A.: 1994b A&A *submitted*

Carney B.W., Seitzer P.: 1993 AJ 105, 2127

Carpenter J.M., Snell R.L., Schloerb F.P.: 1990 ApJ 362, 147

Combes F.: 1991 ARA&A 29, 195

Dame T.M., Elmegreen B.G., Cohen R.S., Thaddeus P.: 1986 ApJ 305, 892

de Geus E.J., Vogel S.N., Digel S.W., Gruendl R.A.: 1993 ApJ 413, L97

Deul E.R.: 1988 Ph.D. Thesis, University of Leiden

Dickman R.L.: 1978 ApJS 37, 407

Digel S.W.: 1991 Ph.D. Thesis, Harvard University

Digel S.W., de Geus E.J., Thaddeus P.: 1994, ApJ *in press*

Dogiel V.A.: 1991 in: Bloemen J.B.G.M. (ed), I.A.U. Symp. 144, p. 175

Elmegreen B.G.: 1989 ApJ 338, 178

Fich M., Blitz L., Stark A.A.: 1989 ApJ 342, 272

Henderson A.P., Jackson P.D., Kerr F.J.: 1982 ApJ 263, 116

Kimeswenger S., Weinberger R.: 1989 A&A 209, 51

Kulkarni S.R., Blitz L., Heiles C.: 1982 ApJ 259, L63

Kutner M.L., Mead K.N.: 1981 ApJ 249, L15

Lequeux J., Allen R.J., Guilloteau S.: 1993 A&A 280, L23

Mathis J.S., Mezger P.G., Panagia N.: 1983 A&A 128, 212

Mead K.N., Kutner M.L.: 1988 ApJ 330, 399

Moffat A.F.J., FitzGerald M.P., Jackson P.D.: 1979 A&AS 38, 197

Robin A.C., Crézé M., Mohan V.: 1992a ApJ 400, L25

Robin A.C., Crézé M., Mohan V.: 1992b A&A 265, 32

Sanders D.B., Scoville N.Z., Tilanus R.P.J., Wang Z., Zhou S.: 1993 in: Holt S.S. & Verter F. (eds), Back to the Galaxy, p. 311

Shaver P., McGee R.X., Newton L.M., et al.: 1983 MNRAS 204, 53

Sodroski J.: 1991 ApJ 366, 95

Solomon P.M., Rivolo A.R., Barrett J., Yahil A.: 1987 ApJ 319, 730

Strong A.W., Bloemen J.B.G.M., Dame T.M., et al.: 1988 A&A 207, 1

Turbide L., Moffat A.F.J.: 1993 AJ 105, 1831

van der Kruit P.C.: 1986 A&A 157, 230

Wilson T.L., Matteucci F.: 1992 A&AR 4, 1

Wouterloot J.G.A., Brand J.: 1989 A&AS 80, 149 (WB89)

Wouterloot J.G.A., Brand J., Burton W.B., Kwee K.K.: 1990 A&A 230, 21